Coulomb excitation of multiphonon levels of the giant dipole resonance

B. F. Bayman
School of Physics and Astronomy, University of Minnesota, 116 Church Street S. E., Minneapolis, Minnesota 55455, USA

F. Zardi
Istituto Nazionale di Fisica Nucleare and Dipartimento di Fisica, Via Marzolo 8, I-35131 Padova, Italy
(Received 19 October 2009; revised manuscript received 22 December 2009; published 17 March 2010)

A closed expression is obtained for the cross-section for Coulomb excitation of levels of the giant dipole resonance of given angular momentum and phonon number. Applications are made to the Goldhaber-Teller and Steinwedel-Jensen descriptions of the resonance at relativistic bombarding energies.

DOI: 10.1103/PhysRevC.81.037901 PACS number(s): 25.70.De, 25.75.−q, 24.30.Cz

The giant dipole resonance (GDR) is one of the best studied collective modes of nuclear excitation. It has been modeled, macroscopically, as a bulk oscillation of neutrons relative to protons [1] or as local isovector fluctuations of neutron and proton fluids [2]. It can also be modeled, microscopically, in terms of isovector linear combinations of particle-hole excitations of the nuclear ground state ([3–5]). It has been studied experimentally using reactions induced by γ rays, light ions, and the sharp pulses of electromagnetic radiation associated with projectile nuclei moving at relativistic speeds, i.e., relativistic Coulomb excitation. In this Brief Report, we will consider relativistic Coulomb excitation of GDR states which are described by macroscopic models.

In many situations, the de Broglie wavelength for the relative motion of the projectile and target in a Coulomb excitation experiment is small compared to the linear dimensions that characterize the system. Then a semiclassical approach can be used, in which this relative motion is described in terms of a classical orbit, whereas the internal changes of the projectile and target are described using quantum mechanics. We are interested in a situation in which the target is excited to the states associated with the GDR. A useful first approximation to an oscillatory situation, such as the GDR, is to assume that the restoring forces are proportional to the displacement from equilibrium. With this approximation, the GDR is dynamically equivalent to an isotropic three-dimensional harmonic oscillator. This assumption leads to the familiar harmonic oscillator spectrum, in which eigenstates are characterized by phonon number, total angular momentum, and angular-momentum z component. If the oscillator picture were exact, all the $(N+1)(N+2)/2$ eigenstates with N phonons would be degenerate in energy. Deviations from the oscillator picture would lift this degeneracy, but if the deviations were spherically symmetric we would still have the $2\ell+1$-fold degeneracy of the angular-momentum eigenstates with $\ell = N, N-2, N-4, \ldots, 0$ or 1.

The coupling between the electromagnetic pulse due to the projectile and the internal oscillating degrees of freedom associated with the GDR of the target can usefully be approximated by an expression that is linear in these oscillating degrees of freedom. If this approximation is made, an exact solution can be found for the Schrödinger equation that describes the time evolution of the target [6,7]. Formulae have been published in the literature for the total excitation probability of all GDR states of given phonon number, when the relative motion of the target and projectile is along a specified orbit. In this Brief Report, we decompose this total excitation probability into the contributions of phonon states of given total angular momentum. For example, we show how to find the excitation probabilities of four-phonon states of angular momentum 0, 2, or 4, whereas the previously published formula yielded only the total four-phonon excitation probability.

These GDR phonon states of specified angular momentum are not clearly resolved in the excitation spectra. Indeed, superposed on the multiphonon GDR states are collective excitations of other characters, such as giant quadrupole and giant octupole excitations (see, e.g., Ref. [3]). Thus we cannot check our predictions for excitation cross sections of GDR states of given angular momentum against any currently available data. However, it is possible that future measurements of angular distributions of the decay products of GDR states will give information about the angular momenta of these states. For example, the γ rays emitted by the $\ell = 0$ member of the two-phonon sextuplet will have a spherically symmetric angular distribution, whereas the five $\ell = 2$ members will emit γ rays with quadrupole and hexadecapole distributions. In situations such as this, it will be important to be able to predict the excitation cross sections of N-phonon states of specified angular momentum.

The perturbed target wave function is expressed as the usual time-dependent linear combination of unperturbed target wave functions ψ_α

$$\Psi(t) = \sum_\alpha a_\alpha(t) e^{-\frac{i}{\hbar}\epsilon_\alpha t}\psi_\alpha, \tag{1}$$

where ϵ_α is the unperturbed target eigenvalue associated with ψ_α. The intial conditions appropriate to a typical nuclear reaction are $a_\alpha(-\infty) = \delta_{\alpha,0}$, corresponding to the requirement that the target be in its ground state at the start of the process. The probability that the reaction leaves the target in the final state ψ_α is then $|a_\alpha(\infty)|^2$.

In a Coulomb excitation reaction, the perturbation experienced by the target is the electromagnetic field due to the passing projectile. Its matrix elements are [8]

$$\langle\psi_\beta|V(t)|\psi_\alpha\rangle = \int\left[\varphi_c^{\rm ret}(\mathbf{r},t)\rho_{\beta\alpha}(\mathbf{r}) - \frac{1}{c}\mathbf{A}_c^{\rm ret}(\mathbf{r},t)\cdot\mathbf{J}_{\beta\alpha}(\mathbf{r})\right]d^3r. \quad (2)$$

Here $\varphi_c^{\rm ret}(\mathbf{r},t)$ and $\mathbf{A}_c^{\rm ret}(\mathbf{r},t)$ are, respectively, the scalar and vector potentials associated with the electromagnetic field created by the charged projectile. The properties of the target states ψ_α and ψ_β are expressed in Eq. (2) by the transition charge density $\rho_{\beta\alpha}(\mathbf{r})$ and current density $\mathbf{J}_{\beta\alpha}(\mathbf{r})$.

In this Brief Report we will be concerned with situations in which the target Hamiltonian is that of an isotropic three-dimensional harmonic oscillator with reduced mass M and natural frequency ω. The labels of the unperturbed states can be taken to be the triplet of quantum numbers (n_x, n_y, n_z), specifying the numbers of oscillator quanta in the x, y, and z directions. Furthermore, we will be working in the regime in which the interaction matrix elements (2) can be approximated by

$$\left\langle\psi_{n_x,n_y,n_z}\middle|V(t)\middle|\psi_{n'_x,n'_y,n'_z}\right\rangle = -\int d^3R\,\psi^*_{n_x,n_y,n_z}(\mathbf{R})[\mathbf{F}(t)\cdot\mathbf{R}+\mathbf{G}(t)\cdot\mathbf{P}]\psi_{n'_x,n'_y,n'_z}(\mathbf{R}) \quad (3)$$

where $\mathbf{R}(=X, Y, Z)$ represents the degrees of freedom undergoing harmonic oscillations and $\mathbf{P}$ represents the conjugate momenta.

The time-dependent Schrodinger equation for the ψ_α, with the perturbation given by Eq. (3), can be solved exactly [6,7]. The result is that the probability of populating the final target state ψ_{n_x,n_y,n_z} is

$$\mathcal{P}_{n_x,n_y,n_z} = \left|a_{n_x,n_y,n_z}(\infty)\right|^2 = \frac{(|\alpha_x|^2)^{n_x}(|\alpha_y|^2)^{n_y}(|\alpha_z|^2)^{n_z}}{n_x!n_y!n_z!}e^{-(|\alpha_x|^2+|\alpha_y|^2+|\alpha_z|^2)} \quad (4)$$

in which the α_j are defined by

$$\alpha_j = i\int_{-\infty}^{\infty}dt'\left[\frac{F_j(t')}{\sqrt{2M\hbar\omega}} + i\sqrt{\frac{M\omega}{2\hbar}}G_j(t')\right]e^{i\omega t'}. \quad (5)$$

Note that this "Poisson distribution" result involves "on-shell" Fourier transforms of $F_j(t)$, $G_j(t)$. These quantities are gauge invariant.

The Cartesian result in Eq. (4) is well known [6]. However specifying the unperturbed eigenstates in terms of n_x, n_y, n_z is not as convenient as using principal and angular-momentum quantum numbers n, ℓ, m. The advantage of using n, ℓ, m is that a spherically symmetric deviation from a perfect harmonic oscillator Hamiltonian will not mix the states labeled by different (ℓ, m), nor will it split the $2\ell+1$ states with different m values and the same ℓ. However, the quantum numbers n_x, n_y, n_z are useful only for a perfect oscillator. Since we cannot expect perfection in a harmonic description of the GDR, but we can expect spherical symmetry, it would be advantageous to use oscillator eigenstates characterized by n, ℓ, m rather than n_x, n_y, n_z.

It is shown in Ref. [9] that the excitation probabilities of all states of given n, ℓ is:

$$\mathcal{P}_{n,\ell} \equiv \sum_{m=-\ell}^{\ell}|\langle n\ell m|\Psi(\infty)\rangle|^2 = \frac{2\ell+1}{(2n)!!(2n+2\ell+1)!!}|(\alpha_x)^2+(\alpha_y)^2+(\alpha_z)^2|^{2n+\ell} \times e^{-(|\alpha_x|^2+|\alpha_y|^2+|\alpha_z|^2)} \times P_\ell\left(\frac{|\alpha_x|^2+|\alpha_y|^2+|\alpha_z|^2}{|(\alpha_x)^2+(\alpha_y)^2+(\alpha_z)^2|}\right), \quad (6)$$

where P_ℓ is a Legendre polynomial. This formula is our main result.

In relativistic Coulomb excitation [10], the projectile linear momentum is very large compared to the transverse impulse the projectile receives as it moves past the target. Then the trajectory of the projectile can be approximated by a straight line, along which the projectile moves with constant speed v, and $\varphi_c^{\rm ret}(\mathbf{r},t)$, $\mathbf{A}^{\rm ret}(\mathbf{r},t)$ are the Lienard-Wiechert potentials [11]. We choose our axes so that the trajectory is parallel to the z axis in the y-z plane. With this choice, $\alpha_x = 0$, α_y is real and α_z is pure imaginary. This is because the influence of the projectile in the z direction is opposite at $\pm t$, whereas its influence in the y direction is the same at $\pm t$. This different time behavior leads to different behavior under complex conjugation of the Fourier transforms that determine α_y, α_z. It is clear that the opposite signs of $(\alpha_y)^2$ and $(\alpha_z)^2$ play an important role in the magnitude of Eq. (6).

In general, α_x, α_y, and α_z will be functions of the impact parameter, b, which characterizes the projectile orbit. Therefore $\mathcal{P}_{n,\ell}$ will also be a function of b. The excitation cross section involves an integral over impact parameter,

$$\sigma_{n,\ell} = 2\pi\int_{b_{\rm min}}^{\infty}\mathcal{P}_{n,\ell}(b)b\,db. \quad (7)$$

The lower limit, $b_{\rm min}$, is of the order of the sum of the radii of the projectile and target nuclei. Because the electromagnetic pulse due to the projectile becomes more adiabatic as b increases, $\mathcal{P}_{n,\ell}(b)$ decreases strongly for large b, and the upper limit of the integral in Eq. (7) can be safely taken to be of the order of a few hundred Fermi.

The Goldhaber-Teller model of the GDR postulates a bulk oscillation of the protons relative to the neutrons. The amplitude of the oscillation is determined by the parameter $\nu \equiv M\omega/\hbar$, where M is the reduced mass associated with the relative oscillation of the proton and neutron mass centers and $\hbar\omega$ is the characteristic energy of the oscillation. For the GDR, the oscillation energy is approximately [12]

$$\hbar\omega \simeq 79A^{-1/3}\ \text{MeV}.$$

Thus

$$\nu = \frac{NZ}{A}m_{\rm p}\frac{\omega}{\hbar} = \frac{NZ}{A}m_{\rm p}c^2\frac{\hbar\omega}{(\hbar c)^2} \simeq \frac{NZ}{A}\times 939\ \text{MeV}\times\frac{79A^{-1/3}\ \text{MeV}}{(197.3\ \text{MeV fm})^2} \simeq 1.91\frac{NZ}{A^{4/3}}\ \text{fm}^{-2}.$$

The amplitude of the oscillation of the proton mass center is then

$$\frac{N}{A} \times \frac{1}{\sqrt{\nu}} \simeq \frac{0.724}{A^{1/3}} \sqrt{\frac{N}{Z}} \text{ fm}. \tag{8}$$

If this distance is small compared to the distance over which the charge density changes by an appreciable fraction of itself, such as the thickness of the nuclear surface, then the linear approximation (3) is applicable, with

$$\mathbf{F}(t) = \frac{N}{A} \int d^3r \varphi_c^{\text{ret}}(\mathbf{r}, t) \nabla_{\mathbf{r}} \rho(\mathbf{r}) \tag{9a}$$

$$\mathbf{G}(t) = \frac{v}{Z m_{\text{p}} c} \int d^3r \mathbf{A}_c^{\text{ret}}(\mathbf{r}, t) \rho(\mathbf{r}) \hat{z}. \tag{9b}$$

Here $\rho(\mathbf{r})$ is the charge density of the protons, with r locating points relative to the proton mass center. To estimate the validity of the approximation (9), let us consider the particular example of a ^{40}Ca target. Then Eq. (8) yields $\simeq$0.212 fm for the amplitude of the oscillation of the proton mass center. Since the proton charge density is approximately constant from its center out to the surface region, whose thickness is approximately 1 fm, we see that the amplitude of the GDR oscillation is indeed small compared to the distance over which the charge density changes by an appreciable fraction of itself.

If Eqs. (5) and (9) are used together with the Lienard-Wiechert potentials, then the $\alpha_x, \alpha_y, \alpha_z$ needed in Eq. (6) can be shown [9] to be

$$\alpha_x = 0 \tag{10a}$$

$$\alpha_y = -i\pi \sqrt{\frac{16N\omega}{m_{\text{p}} Z A \hbar}} \frac{Z_{\text{p}} e^2}{\gamma v^2} K_1\left(\frac{\omega b}{\gamma v}\right) \int_0^\infty j_0\left(\frac{\omega}{c} r\right) \rho(r) r^2 dr \tag{10b}$$

$$\alpha_z = \pi \sqrt{\frac{32N\omega}{m_{\text{p}} Z A \hbar}} \frac{Z_{\text{p}} e^2}{\gamma^2 v^2} K_0\left(\frac{\omega b}{\gamma v}\right) \int_0^\infty j_0\left(\frac{\omega}{c} r\right) \rho(r) r^2 dr. \tag{10c}$$

We have assumed that the proton charge distribution is spherically symmetric.

The Steinwedel-Jensen model of the giant dipole excitation [2] postulates that the protons and neutrons oscillate relative to each other, not in the bulk relative motion of the Goldhaber-Teller model [1] but in local isovector fluctuations. For small fluctuations, we find that

$$\mathbf{F}(t) = -\frac{eNZ}{A^2} n_0 \int d^3r \varphi_c^{\text{ret}}(\mathbf{r}, t) \frac{j_1\left(\frac{\omega}{u} r\right)}{r} \mathbf{r} \tag{11a}$$

$$\mathbf{G}(t) = \frac{v}{Mc^2} \frac{eNZ}{A^2} n_0 \left(\frac{u}{\omega}\right)^2 \int d^3r \varphi_c^{\text{ret}}(\mathbf{r}, t) \nabla \left(\frac{j_1\left(\frac{\omega}{u} r\right)}{r} \mathbf{r}\right), \tag{11b}$$

where n_0 is the equilibrium nucleon number density and u is the fluctuation propagation speed, related to the symmetry energy parameter a_s ($\simeq$23 MeV) by

$$u = \sqrt{\frac{8a_s}{m_{\text{p}}} \frac{NZ}{A^2}}. \tag{12}$$

From Eqs. (5) and (11) we calculate [9]

$$\alpha_x = 0 \tag{13a}$$

$$\alpha_y = -i \frac{8\pi NZ}{A^2} \frac{Z_{\text{p}} e^2 n_0}{\hbar \gamma v} \sqrt{\frac{\hbar}{2M\omega}} K_1\left(\frac{\omega b}{\gamma v}\right) \left[\frac{c}{v} \int_0^R r^2 dr \times j_1\left(\frac{\omega}{u} r\right) j_1\left(\frac{\omega}{c} r\right) - \frac{u}{v} \int_0^R r^2 dr j_2\left(\frac{\omega}{u} r\right) j_2\left(\frac{\omega}{c} r\right)\right] \tag{13b}$$

$$\alpha_z = -\frac{8\pi NZ}{A^2} \frac{Z_{\text{p}} e^2 n_0}{\hbar v} \sqrt{\frac{\hbar}{2M\omega}} K_0\left(\frac{\omega b}{\gamma v}\right) \left[\frac{1}{3} \frac{uv}{c^2} \int_0^R \times j_0\left(\frac{\omega}{u} r\right) j_0\left(\frac{\omega}{c} r\right) r^2 dr - \frac{c}{v} \int_0^R r^2 dr j_1\left(\frac{\omega}{u} r\right) j_1\left(\frac{\omega}{c} r\right) + \frac{2}{3} \frac{u}{v} \left(1 + \frac{1}{2\gamma^2}\right) \int_0^R r^2 dr j_2\left(\frac{\omega}{u} r\right) j_2\left(\frac{\omega}{c} r\right)\right]. \tag{13c}$$

Inspection of both Eqs. (10) and (13) shows that as the bombarding energy increases, α_y approaches a finite limit and α_z approaches zero. The geometry of the collision also requires that $\alpha_x = 0$. In this situation, the argument of the Legendre polynomial in Eq. (6) approaches $|\alpha_y|^2/|(\alpha_y)^2| = 1$, and the excitation probability of a state of specified n, ℓ reduces to the simpler form

$$\mathcal{P}_{n,\ell} \xrightarrow{\gamma \to \infty} \frac{2\ell + 1}{(2n)!!(2n + 2\ell + 1)!!} (|\alpha_y|^2)^{2n+\ell} e^{-|\alpha_y|^2}. \tag{14}$$

Figure 1 illustrates the bombarding-energy dependences of α_y and α_z in the two models. The reaction involves ^{208}Pb projectiles and a ^{40}Ca target. The approach of α_y to a constant limiting value, while α_z strongly decreases, is evident. It is also clear from Fig. 1 that all the cross sections predicted by the Goldhaber-Teller and Steinwedel-Jensen models will be very similar, since all the cross sections are determined by the two parameters α_y and α_z. We get a further simplification of Eq. (14) if we restrict our attention to levels with a given total number of quanta $N = 2n + \ell$. Then we can deduce that

$$\frac{\mathcal{P}_{\frac{N-\ell}{2},\ell}}{\mathcal{P}_{\frac{N-\ell-2}{2},\ell+2}} \xrightarrow{\gamma \to \infty} \frac{(2\ell + 1)(N + \ell + 3)}{(2\ell + 5)(N - \ell)} \xrightarrow{\gamma \to \infty} \frac{\sigma_{\frac{N-\ell}{2},\ell}}{\sigma_{\frac{N-\ell-2}{2},\ell+2}}. \tag{15}$$

The second relation holds because the ratio is independent of α_y and therefore independent of b. According to Eq. (7), if the ratio of excitation probabilities is independent of b, that ratio will also be the cross-section ratio. In the particular case of two-phonon levels, Eq. (15) yields $\sigma_{1,0}/\sigma_{0,2} \xrightarrow{\gamma \to \infty} 1/2$. This is in agreement with the calculation of Bertulani and Baur [6].

Figure 2 shows the bombarding energy dependence of the excitation cross section for levels with four or fewer GDR phonons in a ^{40}Ca target, when the projectile is ^{208}Pb. The calculation was done using the Goldhaber-Teller description of the GDR. As was shown above, the predictions based on the Steinwedel-Jensen description would be similar.

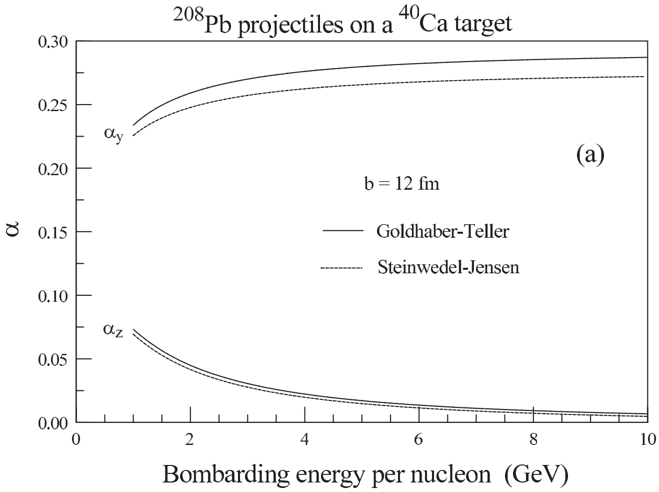

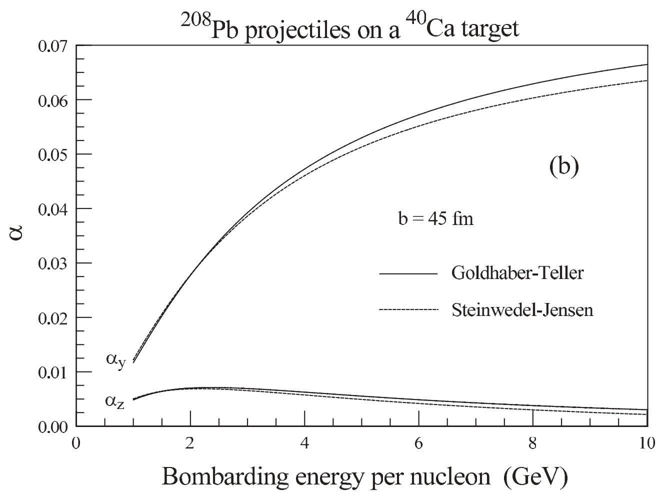

FIG. 1. Comparison of calculations of (α_y, α_z) using the Goldhaber-Teller and Steinwedel-Jensen models of the GDR. (a) $b = 12$ fm; (b) $b = 45$ fm.

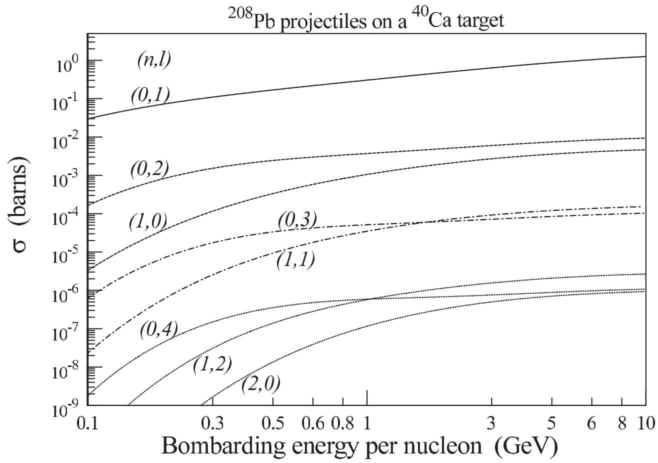

FIG. 2. Excitation cross sections for various (n, ℓ) levels of the GDR in ^{40}Ca, due to Coulomb excitation by ^{208}Pb projectiles. Levels with the same number of phonons are indicated by the same type of line. These calculations are done using the Goldhaber-Teller description of the GDR.

At bombarding energies per nucleon near 10 GeV, Fig. 2 exhibits cross-section ratios consistent with Eq. (15). At lower bombarding energies per nucleon, say below 1 GeV, the cross-section ratios are shown by Fig. 2 to be quite different. Changing the bombarding energy has a significant effect on the ratio of transverse and longitudinal impulses received by the target. It follows from Eq. (6) that this can effect the ratios of excitation probabilities of states of different angular momenta. Indeed, we see that as the bombarding energy per nucleon increases from 1 to 2 GeV, the $N = 2$ and $N = 3$ levels that are most strongly excited change from $\ell = N$ to $\ell = N - 2$. This behavior suggests that some interesting changes in the angular distribution of decay products might be observed as the bombarding energy moves through this region.

[1] M. Goldhaber and E. Teller, Phys. Rev. **74**, 1046 (1948).
[2] H. Steinwedel and J. H. D. Jensen, Phys. Rev. **79**, 1019 (1950).
[3] E. G. Lanza, F. Catara, D. Gambacurta, M. V. Andrés, and Ph. Chomaz, Phys. Rev. C **79**, 054615 (2009).
[4] E. G. Lanza, F. Catara, M. V. Andrés, Ph. Chomaz, M. Fallot, and J. A. Scarpaci, Phys. Rev. C **74**, 064614 (2006).
[5] M. V. Andrés, F. Catara, E. G. Lanza, Ph. Chomaz, M. Fallot, and J. A. Scarpaci, Phys. Rev. C **65**, 014608 (2001).
[6] Carlos A. Bertulani and Gerhard Baur, Phys. Rep. **163**, 299 (1988).
[7] E. Merzbacher, *Quantum Mechanics*, 2nd ed. (John Wiley & Sons, New York, 1970), p. 362.
[8] K. Alder and A. Winther, *Electromagnetic Excitation* (North-Holland, Amsterdam, 1975).
[9] B. F. Bayman and F. Zardi, arXiv:0912.4057 [nucl-th].
[10] A. Winther and K. Alder, Nucl. Phys. A **319**, 518 (1979).
[11] J. D. Jackson, *Classical Electrodynamics*, 3rd ed. (John Wiley & Sons, New York, 1999), p. 662.
[12] A. Bohr and B. R. Mottelson, *Nuclear Structure* (W. A. Benjamin, Inc., Reading, MA, 1975), Vol. II, p. 476.